# Structural Efficiency Study of Graphite-Epoxy Aircraft Rib Structures

Gary D. Swanson* and Zafer Gürdal†
*Virginia Polytechnic Institute and State University, Blacksburg, Virginia 24061*
and
James H. Starnes Jr.‡
*NASA Langley Research Center, Hampton, Virginia 23665*

**The present study focuses on the structural efficiencies of optimally designed composite wing rib panel configurations. The configurations studied include a tailored corrugated panel, a corrugated panel with a constant-thickness continuous laminate, and a hat-stiffened panel. Also included in the study are a blade-stiffened panel and a flat unstiffened plate which are used as baseline configurations for comparison. Thicknesses of different plies with preselected ply orientations in the different sections of the panels and detailed cross-sectional dimensions are used as sizing variables. The constraints considered include those associated with material strength, buckling, and geometric limits. The loads considered for this study are based on a typical loading of an inboard wing rib fuel cell closeout panel for a large transport aircraft and include in-plane axial compression $N_x$, shear $N_{xy}$, and out-of-plane pressure $P$. Structural efficiencies and cross-sectional geometries of different configurations are compared for a wide range of combined loads. Transition of the optimal cross-sectional geometry from one panel configuration to another is demonstrated as the loading is varied. The sensitivities of optimized designs to large changes in some of the geometric parameters are also studied.**

## Introduction

BECAUSE of their high acquisition costs and more complex design and analysis requirements compared to similar metallic structures, application of composite materials to large transport aircraft has been mostly limited to secondary structures such as fairings and control surfaces. Although these composite secondary structures have saved weight compared to their metallic counterparts, they account for only a small fraction of the total structural weight of an aircraft. In order to obtain maximum weight savings that will significantly increase aircraft performance, application of composite materials must be considered for primary aircraft structures such as the wing, fuselage, and empennage. Because of the large size and high cost of a transport aircraft, a dedicated effort to determine the best design configurations and cost-effective fabrication techniques for large primary structures is required.

A detailed review of earlier research efforts on analysis, design, and structural efficiencies of a variety of stiffened panel configurations for primary aircraft structures has been presented in Ref. 1. The present study focuses on the structural efficiencies of optimally designed composite wing rib panel configurations with economical manufacturing possibilities. Aircraft wing rib panels exhibit some characteristics that are not common to many structural panels. One of the major differences between a wing rib panel and other structural panels is its aspect ratio. More specifically, wing rib panels are short in length (measured in the wing thickness direction) compared to their width (measured in the chordwise direction). Earlier design studies found in the literature mostly concentrated on nearly square structural panels. Also, some of the rib panels in a wing are commonly used as fuel cell closeout panels and, therefore, are subjected to out-of-plane pressure loads in addition to the in-plane axial compressive and shear loads resulting from the wing bending and torsion under aerodynamic loads. The present paper presents the results of a study of minimum-weight panel designs that satisfy buckling and strength constraints for wing rib panels subjected to a wide range of combined in-plane and out-of-plane load conditions.

## Panel Configurations and Design Approach

The baseline model considered for a wing rib panel is that of a center wing box fuel cell closeout rib of a typical large transport aircraft. The rib dimensions used are 28 in. high by 80 in. wide. The panel configurations are chosen to be practical and applicable to cost-effective manufacturing techniques. These configurations are shown in Fig. 1, and include a tailored corrugated panel with different laminate thicknesses for crowns and webs, a corrugated panel with a continuous constant-thickness laminate throughout its length and width, and a hat-stiffened panel. A corrugated panel is relatively easy to manufacture since it has continuous plies that run throughout the configuration that form integral stiffeners without requiring fasteners. It is also suitable for the thermoforming process that is a potentially economical fabrication technique for thermoplastic materials. Also included in the study are a blade-stiffened panel, which is the most commonly used concept considered for wing rib applications, and a flat unstiffened plate, which is used as a baseline configuration for comparison.

The constraints considered in the present study include those associated with material strength, buckling, and geometric limits. The material-failure criterion chosen is the maximum strain-failure criterion. The buckling criterion used in the present study is based on the common design practice used for wing structures, which does not allow the components to buckle at design loads. Thus, the design of the wing

Received April 26, 1990; revision received May 23, 1990; accepted for publication May 29, 1990. 

*Graduate Student; currently Structural Design Engineer, Boeing Commercial Airplane.
†Associate Professor, Department of Engineering Science and Mechanics. Member AIAA.
‡Head, Aircraft Structures Branch. Associate Fellow AIAA.

rib does not consider any postbuckling load-carrying capability of the panel.

The design variables considered in the present study are the thicknesses of different plies with preselected ply orientations in the different sections of the panels. The ply angles are chosen as fixed conventional values that consist of ±45-, 0-, and 90-deg ply orientations. Also, detailed cross-sectional dimensions are used as sizing variables to determine the best cross-sectional geometry. Hercules AS4/3502 preimpregnated graphite-epoxy tape was chosen as a typical graphite-epoxy material and is the only material considered for this study. Mechanical properties for this graphite-epoxy material are $18.50 \times 10^6$ psi for longitudinal Young's modulus; $1.89 \times 10^6$ psi for transverse modulus; $0.87 \times 10^6$ psi for in-plane shear modulus; and 0.30 for major Poisson's ratio.

**Design and Analysis Tools**

The Panel Analysis and Sizing Code[2,3] (PASCO) was chosen as the primary sizing and analysis tool for this study. PASCO consists of a buckling-analysis program, VIPASA,[4] and an optimizer, CONMIN,[5] and has the capability to model the panel configurations and load conditions considered and to apply the design constraints of interest. PASCO is computationally efficient, which allows the large number of design cases required for a study of this nature to be performed at a reasonable computational cost. One drawback of using PASCO for this study is its potential for inaccurately modeling the boundary conditions. Boundary conditions on the panel ends perpendicular to the stiffeners are assumed to be simply supported and cannot be changed in PASCO. This simple support boundary condition is inherent in the PASCO analysis for an orthotropic plate with no applied shear and is considered accurate in the sense that it is the exact solution of the plate equations satisfying the Kirchhoff-Love hypothesis. Without the shearing loads, the buckling pattern consists of a series of straight nodal lines that are parallel to the loaded edges of the panel. When shear is applied to the panels, the buckling pattern consists of a series of skewed nodal lines, as shown in Fig. 2, and the buckling load calculated for this load case may not correspond to the buckling load of a simply supported plate. This is especially true if a single buckling half-wave of length $\lambda$ forms along the panel length $L$, in which case the PASCO analysis can severely underestimate the buckling load. For the short rib panels subjected to the combined loads considered in this study, a single half-wave buckling mode may occur and, therefore, PASCO designs may need to be corrected.

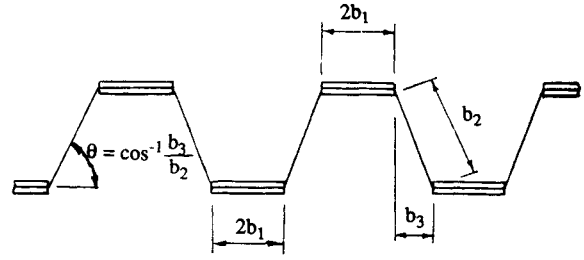


a) Tailored corrugated panel

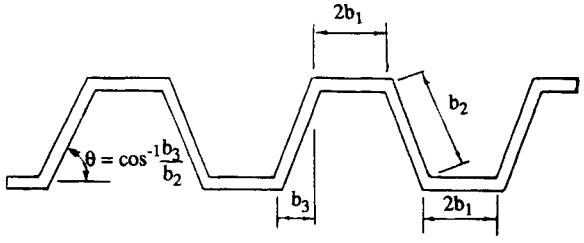


b) Corrugated panel with a continuous laminate

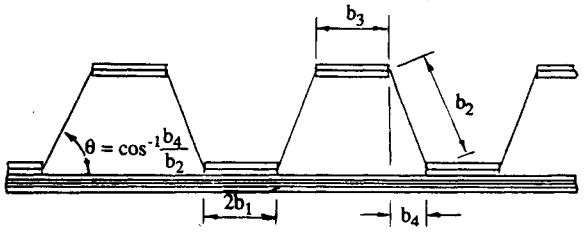


c) Hat-stiffened panel

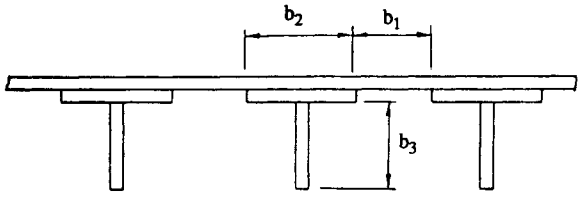


d) Blade-stiffened panel

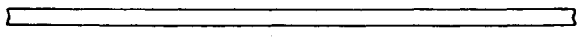

e) Unstiffened flat plate

**Fig. 1 Configurations studied.**

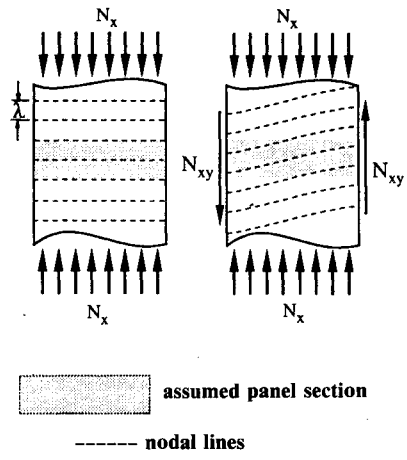


**Fig. 2 PASCO skewed buckling nodes due to applied shear.[3]**

An optional smeared-stiffness solution is included in PASCO for the $\lambda = L$ buckling load to provide a more accurate solution when a shear load is present.[3] The smeared-stiffness approach was shown[6] to be an improved solution, but not always a conservative one. Additionally, in order to obtain an optimally designed stiffened panel configuration, the full cross-sectional detail must be retained to account for local stiffener buckling, while maintaining the simple support boundary conditions at the loaded edges. The smeared-stiffener solution in PASCO does not account for this detail and, therefore, a recently developed computer program VICON, VIPASA with constraints,[7,8] is used. VICON modifies the VIPASA buckling-analysis program to include support points with no out-of-plane deflection at preselected locations on the panel. By specifying rows of support points along the panel width at intervals corresponding to the ends of the desired panel length, the simple support boundary conditions at the panel ends can be enforced when shear is applied.

In order to include the modifications of the VICON analysis in the PASCO design, a two-step iterative process is used. PASCO is used to generate a design based on the smeared-orthotropic stiffness solution, which is then analyzed using VICON. The design load for PASCO is then reduced by the ratio of the original PASCO design load to the VICON buckling load for the overall buckling mode, $\lambda = L$. The panel is redesigned using PASCO with this correction for the overall buckling load and the resulting design is again checked using VICON. This iterative process is continued until the analyses converge.

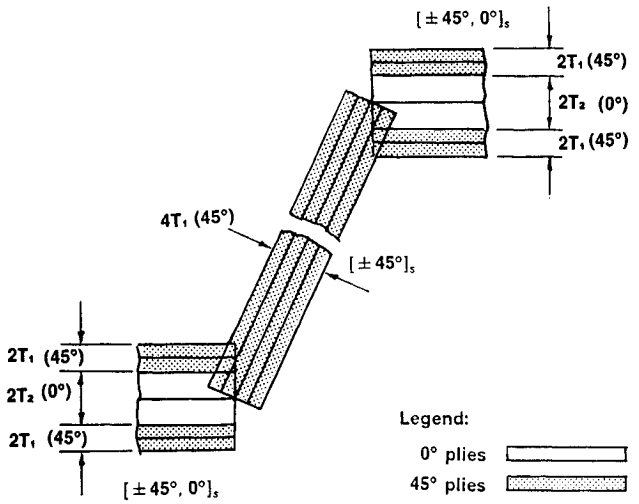


**Fig. 3 Tailored corrugated panel model.**

*PASCO Models*

The geometry of the repeating elements used to model the panel is typically defined by the plate-element width design variables $b_1$–$b_4$ as shown in Fig. 1. Both the upper and lower corrugation caps for the corrugated panels are assumed to be of equal width. The plate-element widths, $b_2$ and $b_3$, define the corrugated panel web angle $\theta$. The panel webs are made of only ±45-deg plies (see Fig. 3) that run continuously across the width of the cross section. Such continuous plies help to reduce both manufacturing costs and any stress concentrations that occur at the ±45-deg ply termination points. In the plate elements that make up the caps, 0-deg plies are included between the layers of ±45-deg fibers. Thus, the entire laminate is defined by two thickness design variables, indicated as $T_1$ and $T_2$ in Fig. 3, relating to the ±45-deg and 0-deg plies, respectively.

The corrugated panel with a continuous laminate is modeled in a similar manner to the tailored corrugated panel, except that all of the plate elements are made up of a symmetric laminate with a sequence of ±45-, 0-, and 90-deg plies. The same quantities that are used to define the cross-sectional geometry for the tailored corrugated panel and the thicknesses of the individual plies are used as design variables.

The hat-stiffened panel is essentially a tailored corrugated panel described above attached to a flat face sheet. The cap widths in the corrugated panels are no longer equal since the geometry of the hat-stiffened panel is not symmetric about the panel midplane. The skin elements are made up of a symmetric laminate with ±45-, 0-, and 90-deg plies. The thicknesses of the individual plies in the skin laminates and the width of the attachment flange of the corrugation are additional design variables.

The blade-stiffened panel is defined by three independent laminates. The skin panel is a symmetric laminate with ±45-, 0-, and 90-deg plies. The flange of the blade stiffener is also a symmetric laminate with ±45-, 0-, and 90-deg plies, and one-half of the laminate extends into the blade stiffener. The laminate defining the blade is made up of a symmetric laminate with a sequence of ±45-, 0-, 90-, ±45-, and 0-deg plies where the first ±45-, 0-, and 90-deg plies are continuous from the flange. The additional ±45- and 0-deg plies allow the blade properties to be different from that of the flange properties. The unstiffened flat-plate configuration is defined by a symmetric laminate with ±45-, 0-, and 90-deg plies of various thicknesses.

For load cases that involve out-of-plane pressure loads, the panel models described above must be modified. PASCO accounts for the lateral pressure by applying a bending moment to the panel that results in a variation in the longitudinal stresses across the thickness of the cross section. Since the individual plate elements in PASCO can carry only constant in-plane loads, the panel models must be modified to account for the variation of the in-plane loads across the corrugation web (or the blade height). This modification is achieved by replacing the single-plate element representing the corrugation web (or the blade) with three linked plate elements with equal thicknesses.

*Design Loads*

The magnitudes of the in-plane axial compression $N_x$, shear $N_{xy}$, and pressure $P$ loads selected for this study are based on a typical loading of an inboard wing rib fuel closeout cell for a large transport aircraft. A load index of $N_x/L$ with values ranging from 0.3 to 1000 psi, where $L$ is the panel length, is used to define the axial compression loads. This range represents an additional loading above and below the typical rib loads so that design trends for panels for other subcomponents, such as a wing skin, are covered.[9,10] The range of applied shear $N_{xy}$ is chosen to be a fraction of the applied axial compression load. Shear load to axial compression load ratios $N_{xy}/N_x = 0.0$, 0.3, 0.6, and 1.0 are investigated. Even though a pressure of $P = 15$ psi is considered to be typical fuel pressure, peak pressures due to maneuvering fuel sloshing or impact can be considerably higher. Thus, values of applied pressure up to 45 psi are considered.

## Design Study Results

Effects of the various load conditions on the geometry and individual lamina thicknesses of the panels are determined and the results are presented in the form of standard structural-efficiency charts and diagrams showing the detailed cross-sectional geometries of the repeating elements that make up the panel cross section. The structural-efficiency charts show the weight index $W/LA$ as a function of the applied axial load index $N_x/L$, where $W$ is the panel weight and $A$ is the panel area. These curves represent a series of designs which form a lower bound of weight for a given panel configuration designed to carry the indicated load. The curves are generated by determining the minimum-weight design for

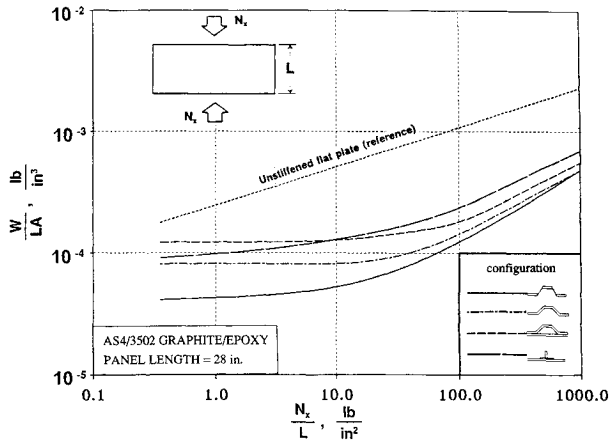


**Fig. 4 Structural efficiency curves for axial compression loaded panels.**

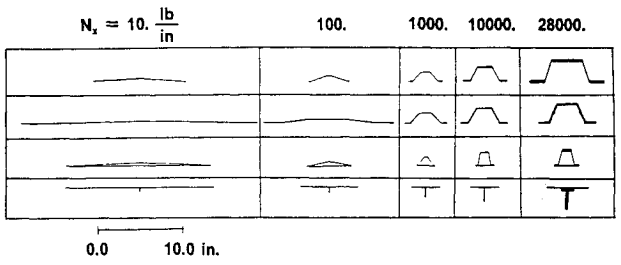


**Fig. 5 Geometry of axial compression loaded panels.**

several different values of the loading parameters, and a curve is fitted to these data points using a cubic spline. Different load combinations are treated separately, and results for each case are presented in the following sections. The results presented are for 80-in.-wide panels. The height of the panels are mostly 28 in., which are marked on all of the structural-efficiency charts.

### Axial Compressive Loading

Panel designs for pure axial compression loads are generated by using PASCO alone. The effect of axial compression load intensity on the structural efficiency and geometry of all of the panel configurations considered in the present study is shown in Figs. 4 and 5, respectively.

*Lightly Loaded Panels*

In the load range $N_x/L$ less than 100 psi, the tailored corrugated panel is noticeably more efficient than the other configurations (see Fig. 4). For example, for $N_x/L = 1.0$ psi, the tailored corrugated panel is nearly half the weight of the corrugated panel with a continuous laminate, slightly less than half the weight of the blade-stiffened panel, and almost one-third of the weight of the hat-stiffened panel. These large weight differences are largely due to the modeling of the laminates that define the panel geometry. Each configuration is modeled such that the minimum number of plies necessary to define the geometry are used, and this number differs for each model. For a low axial load intensity, all of these configurations, excluding the unstiffened flat plate, are constrained by the same minimum gauge ply thickness of 0.005 in. on all of the plies. Therefore, the weight of a panel is almost directly proportional to the number of layers in the cross section and is independent of the intensity of the load. For an axial load of $N_x/L = 1.0$ psi, for example, the tailored corrugated panel consists of four plies, the corrugated panel, with a continuous laminate consists of eight plies, the blade-stiffened panel consists of 8 plies, and the hat-stiffened panel consists of 10 plies.

The optimum geometry of the tailored corrugated panel in this load range consists of a minimum ply thickness $(\pm 45 \text{ deg})_s$ laminate with small regular bends along its width and diminished caps (see Fig. 5). This configuration will hereafter be referred to as a bent-plate design. Further analysis of the optimum bent-plate design revealed that the local buckling (buckling of the individual bend sections) and the global buckling modes of the plate occur simultaneously. This modal interaction between the global and local buckling modes is expected to reduce the buckling load in practical applications and, therefore, the designers may need to impose constraints to prevent simultaneous local and global modes from occurring. Also, a slight change in the bend angle for small angles is observed to change the buckling load significantly, thus, indicating a high sensitivity of this configuration to changes in the geometry and loading conditions. The bent-plate configuration is of particular interest because of the possibility of adopting a simple manufacturing method for production. This same bent-plate configuration, with a flat face sheet attached, essentially describes the geometry of lightly loaded hat-stiffened panels.

For loads approaching $N_x/L = 10.0$ psi, the tailored corrugated panel and the blade-stiffened panel both show some increase in structural weight, even though the laminates all remain constrained by minimum-gauge ply thicknesses. The weight increase for the tailored corrugated panel is attributed to changes in the optimum corrugation angle. The increase in the blade-stiffened panel weight can be attributed to the decreased spacing of the stiffeners and the slight increase in the stiffener height. These geometry changes in the blade-stiffened panel essentially add material to the panel as opposed to the other configurations, which basically change their geometrical configuration. For axial compressive loads larger than $N_x/L = 10.0$ psi, the blade-stiffened panel is the least efficient configuration.

In the load range between $N_x/L = 10$ and 100 psi, each of the configurations undergoes cross-sectional geometry changes associated with decreased repeating element widths, and increased stiffener depths, while the optimum individual ply thicknesses remain at the minimum ply thickness. The tailored corrugated panel at $N_x/L = 100$ psi is still a bent-plate design with larger bend angles. These changes in the cross-sectional geometry cause different amounts of weight increase for different configurations for this moderate increase in load. For example, the tailored corrugated panel, the blade-stiffened panel, corrugated panel with a continuous laminate, and the hat-stiffened panel increase their weights by 141, 85, 83, and 38%, respectively.

*Heavily Loaded Panels*

For $N_x/L$ above 200 psi, the minimum-gauge ply thickness constraints are no longer active, and the structural weight indices $(W/LA)$ of the panel configurations become larger with increased loads. For loads near $N_x/L = 1000$ psi, both the material-failure constraint and the buckling constraint are active for the optimum design. The cross-sectional geometries, Fig. 5, show an increased thickness of 0-deg fibers in the caps of the tailored corrugated panel and the hat-stiffened panel, an increased stiffener thickness in the blade-stiffened panel, and an increased laminate thickness in the corrugated panel with a continuous laminate. For loads above $N_x/L = 200$ psi, the structural efficiencies of the panels are similar, with the tailored corrugated panel and the corrugated panel with a continuous laminate approaching the same weight near $N_x/L = 1000$ psi (see Fig. 4).

### Axial Compression and Pressure Loads

PASCO uses a beam-column approach to account for the interaction of the in-plane loads with the out-of-plane pressure load.[3] The effect of the interaction is included during the analysis as a moment applied at the loaded ends of the panel. The applied moment is equivalent to a maximum moment that occurs at the midspan of a uniformly loaded beam. The effect of this applied moment on panel design is to force the sizing code to increase the overall buckling load corresponding to $\lambda = L$ to be a noncritical value, which, in turn, causes local buckling of web elements to become critical. The increase in the overall buckling load is due to the increase in panel thicknesses required to resist the bending strains induced by the pressure loading.

This very important load condition was often neglected in previous studies. However, since PASCO includes pressure effects only through added bending loads, a level of approximation is made that does not consider any nonlinear effects,

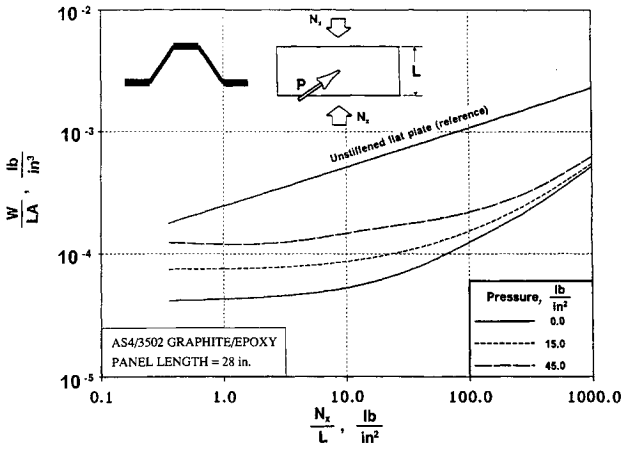


**Fig. 6 Structural efficiency curves of a tailored corrugated panel loaded in combined pressure and axial compression.**

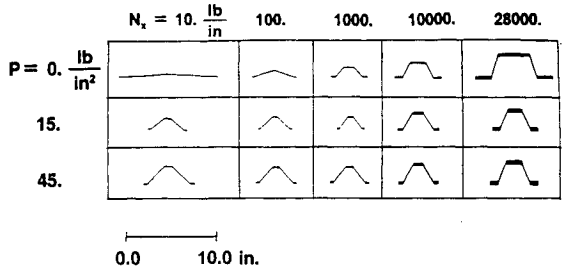


**Fig. 7 Geometry of tailored corrugated panels loaded in combined pressure and axial compression.**

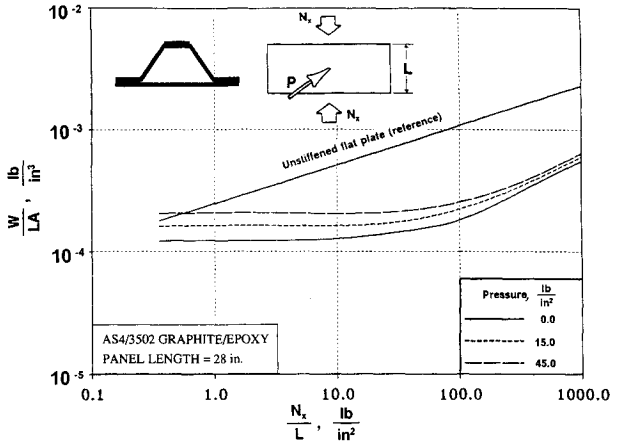


**Fig. 8 Structural efficiency curves of a hat-stiffened panel loaded in combined pressure and axial compression.**

and the final design must be verified with a detailed analysis, which is not included in the present paper. The effects of this load combination on the efficiency and cross-sectional geometry of each of the configurations are discussed in the following sections.

*Tailored Corrugated Panel*

The effect of lateral pressure is most pronounced at the low end of the load range causing the structural weight index to increase substantially as shown in Fig. 6. Specifically, for $N_x/L = 1.0$ psi, an applied pressure of 45 psi increased the structural weight 190% above a panel designed without the applied pressure. The effect of lateral pressure on the geometry is shown in Fig. 7. The most dramatic geometry changes occur at the lower pressure levels, with $P$ less than 15 psi. There is little bending stiffness in the panel designed without the applied pressure; therefore, the moment due to even a small amount of applied pressure causes a noticeable change in the geometry to create the bending stiffness needed to carry the additional moment. In general, for increasing pressure levels the web angle and cap width increase, while the repeating element width decreases. The moment also activates the material-strength constraints which, in turn, result in some increase in the ply thicknesses. Combined geometry changes and the ply thickness increases are the cause of the weight increases. For low axial compression load levels, as the magnitude of the applied pressure increases, the rate of increase in weight for each unit of pressure increase becomes smaller. That is, once the geometry is adjusted to account for the small pressure load, further increase in applied pressure causes only thickness increases with smaller weight penalties.

For panels loaded by heavy axial compression loads, $N_x/L$ greater than 1000 psi, any increase in pressure has only a small effect on the weight parameter. Specifically, for $N_x/L = 1000$ psi, an applied pressure of 45 psi increases the structural weight by only 20% over a panel designed without pressure. The reduced sensitivity of highly loaded panels to pressure changes indicates the existence of sufficient bending stiffness in those high axial compression loaded panels so that only relatively small changes in the cross-sectional geometry and ply thicknesses are needed. The geometry for $N_x/L = 1000$ psi has smaller repeating element widths than the panel designed without pressure for applied pressures of up to 15 psi but changes little for pressures above that value.

*Corrugated Panel with a Continuous Laminate*

Although the continuous laminate corrugated panel is heavier than the tailored corrugated panel at the lower load levels due to minimum-gauge constraints, the structural efficiency and the geometry of both configurations respond to increasing amounts of applied pressure in a similar manner. For higher axial loads near $N_x/L = 1000$ psi, the structural efficiencies of both configurations are very close to one another and, as the intensity of the pressure is increased at this higher load level, only small changes in the structural efficiency of the continuous corrugated laminate are observed. The similarity between the corrugated panels with tailored and continuous laminates leads to the conclusion that the highly loaded corrugated panels, in general, are insensitive to changes in the laminate properties of the individual walls, and changes in the laminates may alter the stress distribution within the cross section without a severe weight penalty.

*Hat-Stiffened Panel*

The effect of applied pressure on the structural efficiency of this configuration is shown in Fig. 8. Similar to the previous configurations, for a lightly loaded panel, even a small amount of applied pressure causes the weight to increase. This increase, however, is less than the increase observed at the same load level for the corrugated panels. The weight of the panel increases 75%, for example, for $N_x/L = 1.0$ psi, as the applied pressure is increased from 0 to 45 psi. At the high load levels near $N_x/L = 1000$ psi, only an 18% weight increase is observed for the same pressure increase. The changes in the hat-stiffened panel geometry, shown in Fig. 9, are

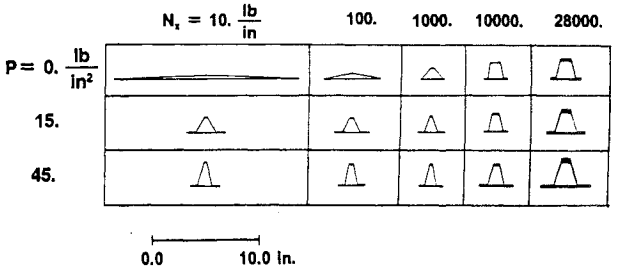


**Fig. 9 Geometry of hat-stiffened panel loaded in combined pressure and axial compression.**

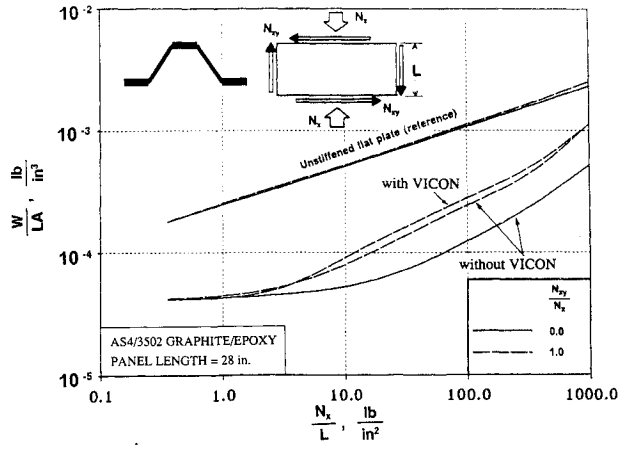


**Fig. 10 Structural efficiency curves for a tailored corrugated panel loaded in combined axial compression and shear.**

similar to the changes in the corrugated panel configurations mentioned previously for increased load intensities. For the lightly loaded panels, an applied pressure load of up to 15 psi results in significant changes in the geometry, such as reduced repeating element widths and deeper hats. As the pressure is increased beyond 15 psi, the cross-sectional geometry is affected less. For the very high load levels near $N_x/L = 1000$ psi, only some increase is observed in ply thickness in the caps and skin to account for the active material-failure constraint. For this configuration, the spacing between hats, where the skin and stiffeners are attached, is not calculated based on a rigorous analysis in the present study (only a minimum plate-element width is imposed to keep a zero plate width from occurring), and for many cases, this dimension appears unreasonably small. A more detailed study to assure the integrity of the attachment of the components is necessary.

*Blade-Stiffened Panel*

The blade-stiffened panel, in general, follows the trends set by the previously described configurations, both in structural efficiency and geometry. Increasing the pressure from 0 to 45 psi for $N_x/L = 1.0$ psi results in nearly a 200% increase in weight. At light load levels ($N_x/L$ less than 10 psi), when no pressure is applied, the panel is designed with small, widely spaced stiffeners. When the pressure is applied to this lightly loaded design, the stiffener spacing decreases significantly and each stiffener increases its depth. For heavily loaded panels, the design changes in the configuration due to the applied pressure are less noticeable. Increasing the applied pressure from 0 to 45 psi at $N_x/L = 1000$ psi results in only a 14% structural weight increase.

**Axial Compression and Shear Loading**

As mentioned earlier, PASCO and VICON are used together iteratively to improve the accuracy of the calculated overall buckling load in the PASCO analysis when shear is applied. The VICON correction is of interest because it provides a better estimate to the overall buckling load in the presence of applied shear than the PASCO solution obtained with the optional smeared orthotropic stiffness method.

*Tailored Corrugated Panel*

Structural efficiencies of corrugated panels with optimally tailored laminates loaded by shear loads along with an axial compressive load are presented in Fig. 10 for $N_{xy}/N_x = 0.0$ and 1.0. Details of designs with intermediate values of shear-load-to-axial-load ratios are given in Ref. 1. Panels designed with PASCO alone show little change in structural efficiency due to shear at the lower applied loads of $N_x/L$ less than 5 psi, where minimum-gauge constraints are active. For axial compression loads greater than 5 psi, the shear load causes a significant weight increase compared to plates loaded under pure axial compression.

The buckling loads calculated by the PASCO and the VICON analyses deviate from one another for axial load levels greater than 10 psi, where the minimum-gauge constraints are inactive and the buckling constraints begin to govern the design. The VICON corrected designs are consistently 15% heavier than the PASCO designs in the axial load range from 10 to 200 psi. The VICON corrections in this load range have an effect on structural efficiency even for low values of $N_{xy}/N_x$ ratios. At the high end of the load range near $N_x/L = 1000$ psi, the material-failure constraints are critical and the effect of the VICON corrections on the structural efficiency becomes insignificant.

Changes in the geometry of the repeating elements as a result of combined axial compression and applied shear loads are presented in Fig. 11 for the tailored corrugated panels (designed both with and without the VICON correction) for $N_{xy}/N_x = 1.0$. For lightly loaded panels where the minimum-gauge constraint is active, the effect of increasing shear on the

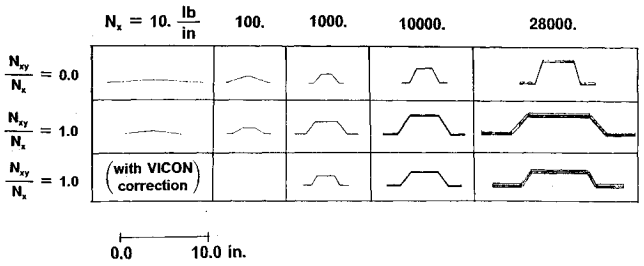


**Fig. 11 Geometry of tailored corrugated panels loaded in combined axial compression and shear.**

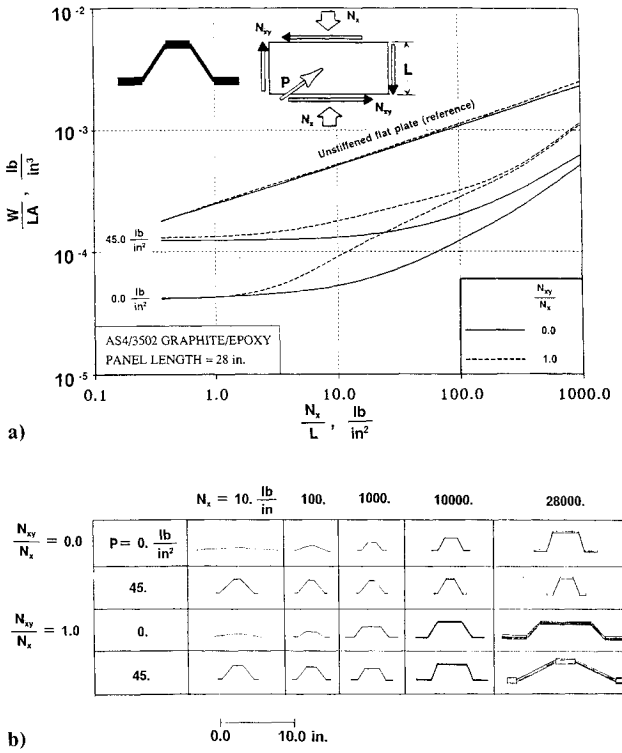


**Fig. 12 Tailored corrugated panel loaded in combined axial compression, shear and pressure: a) structural efficiency; and b) geometry.**

designs is minor regardless of the VICON correction. The width of the repeating element decreases and the corrugation angle of the bent plate increases slightly. For the higher axial loads ($N_x/L$ greater than 100 psi), the application of shear increases the repeating element width, reduces the web angles, increases the cap widths, and increases the ply thicknesses for both the 0- and $\pm$45-deg plies. The wider cap widths may be attributed to the tendency of an individual plate element with a larger aspect ratio to carry larger shearing loads. For such high loads, the effect of the VICON correction on the geometry is noticeable when compared to the PASCO design and results in panel designs that have relatively narrow repeating element widths and shallower corrugation depths.

*Corrugated Panel with a Continuous Laminate*

For the corrugated panel with a continuous laminate, the VICON corrections are assumed to be similar to the corrections for the corrugated panel with tailored laminates. The effect of shear on the structural efficiency and on the geometry of the corrugated panel with a continuous laminate is very similar to the effect on the tailored corrugated panels designed by using PASCO. At low axial compression load levels, the additional shear load does not cause an increase in weight. As the load increases to $N_x/L = 1000$ psi, the structural efficiency of the panel approaches the structural efficiency of the tai-

lored corrugated panel for each level of applied shear load. The 90-deg ply in the laminate, which is not included in the tailored configuration, remains at minimum gauge for all load levels.

*Hat- and Blade-Stiffened Panels*

The effect of the shear load on the structural efficiency and geometry of the hat- and blade-stiffened panel configurations is, in general, similar to those described earlier for the two corrugated panel geometries. For these configurations, the addition of shear causes a slight increase in weight due to minor adjustments in the geometry only at the higher end of the load range. For a shear load ratio of $N_{xy}/N_x = 1.0$ and low axial compression loads, the geometric effects of the additional shear load on the blade-stiffened panel is to decrease the repeating element widths and to increase the blade height while the ply thicknesses remain at minimum-gauge thickness. These geometric trends hold until an increased axial load near $N_x/L = 100$ psi causes the minimum-gauge constraints to become inactive. The VICON corrections to the analysis have little effect on the structural efficiency and on the cross-sectional geometry of both configurations over the entire load range.

**Axial Compression, Shear, and Pressure Loading**

The results of applying a combination of axial compression, shear, and out-of-plane pressure loads to the panel configurations, using the smeared orthotropic stiffness solution in PASCO, are presented in the following sections. Ideally, for the design of a panel under combined axial compression, shear, and pressure, the global buckling loads must be corrected (using VICON, for example) to account for the skewed mode shapes resulting from the shearing loads. However, since the overall buckling mode in the PASCO analysis is not critical for designs in which pressure is applied, the error in the global buckling analysis only affects the panel design through the magnification factor which is used to calculate the applied moment resulting from the out-of-plane pressure. The VICON correction for this moment was found to have little effect on the design trends.

*Tailored Corrugated Panel*

The results for the combined loading of axial compression, shear, and lateral pressure for the tailored corrugated panel are shown in Fig. 12 for pressure levels of 0 and 45 psi and for shear levels of $N_{xy}/N_x = 0.0$ and 1.0. The trends for the structural weight for various combinations of pressure plus compression and shear loads for all values of $N_{xy}/N_x$ ratios are similar to those for the effect of pressure and axial compression alone. Likewise, the effect of shear plus axial compression and pressure on structural weight and configuration is similar for all pressure levels to the trends discussed for the effect of shear on panels loaded in axial compression without pressure. However, the pressure load causes an increase in stiffener height and a decrease in stiffener spacing.

The effects of combined loads on design trends of other structural configurations are similar to the trends of the tailored corrugated panel discussed previously. A detailed description of ply thicknesses and other cross-sectional dimensions for those configurations is given in Ref. 1, which also includes the results for some intermediate pressure and shear levels that are not presented herein.

## Design Sensitivities

Many factors associated with the design and manufacturing of a stiffened panel can affect its expected performance level. To better identify the factors that are most critical, the sensitivity of the structural efficiency to changes in optimum geometric design parameters is studied. Some of the changes in design parameters from their optimum values are minor and can be attributed to manufacturing errors or limitations. The effect of such small variation on the optimum structural efficiency was shown in Ref. 6 to be small. However, in some cases, additional constraints (such as functional requirements and practical limitations in the manufacturing and design process) may force the panel dimensions to be significantly different from the optimum dimensions. For example, an access hole in a rib panel may force the stiffener spacing to be a large nonoptimum value. In the case of a hat-stiffened panel, the width of the corrugation crown attached to the face sheet may be dictated by the magnitude of interlaminar stresses in the attachment flange region. Such a consideration may require the spacing between the corrugations to be a large nonoptimum value. A discussion of the effect of such large changes on the panel weight and cross-sectional details follows. The approach used is to redesign the panels by fixing a particular design variable to a nonoptimum value and then letting the optimizer determine new values of the other design variables that will minimize the weight. This approach is used in order to assure that the effect of large changes in design variables on structural performance is minimized, rather than simply performing a single analysis of the optimum design by changing the value of a single variable to a nonoptimum value. The same approach is also used for small variations in some of the design variables.

**Cross-Sectional Changes**

First, the results of imposing changes on the spacing between the stiffening elements of the corrugated, hat-stiffened, and blade-stiffened plates are discussed. For the optimum corrugated panel geometry, the upper and lower cap widths of the corrugation are equal, creating symmetry about the midplane of the cross section. Forcing a large spacing between small corrugations creates a new geometry that is often referred to as a bead-stiffened panel configuration, where the ratio of the distance between corrugations to the corrugation width itself is referred to as bead ratio. A similar configuration is also possible for the hat-stiffened panels. For illustra-

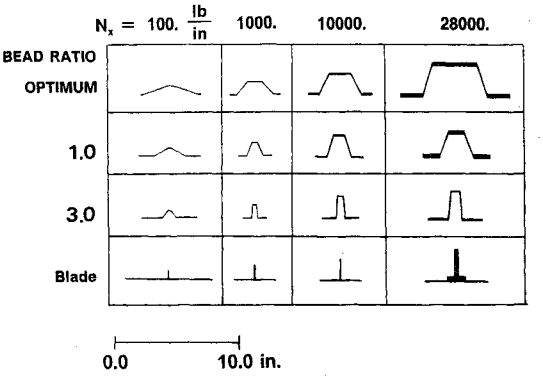


**Fig. 13 Beading effect on corrugated panel geometry.**

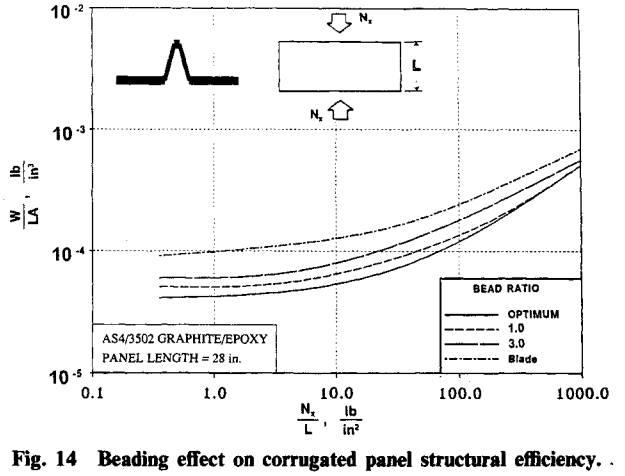


**Fig. 14 Beading effect on corrugated panel structural efficiency.**

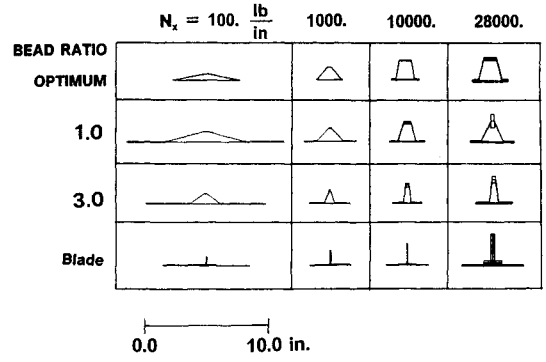


**Fig. 15 Beading effect on hat-stiffened panel geometry.**

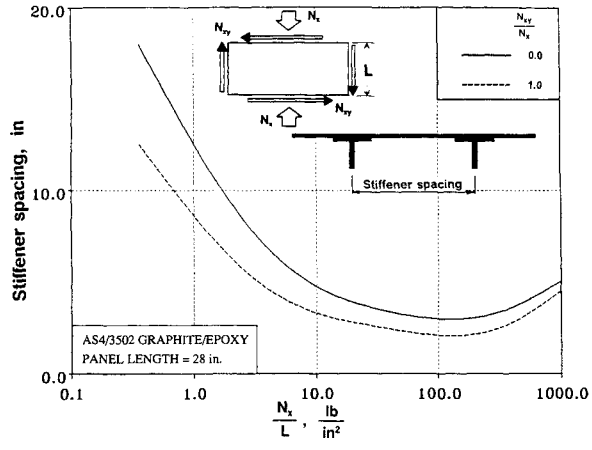


**Fig. 16 Effect of axial compression and shear loads on optimum stiffener spacing of blade-stiffened panels.**

tion, the effect of bead stiffeners on the panel performance for the tailored corrugated panel and for the hat-stiffened panel with bead ratios of 1.0, 3.0, and 10.0 are presented for combinations of in-plane axial compression and shear loads. Also presented are panel designs with imposed nonoptimally spaced blade stiffeners.

*Bead-Stiffened Panels Subjected to Axial Compression Loads*

The cross-sectional geometries and structural efficiencies of the tailored corrugated bead-stiffened panel configurations subjected to various axial compression loads are presented in Figs. 13 and 14, respectively, along with the optimum blade-stiffened panel results for comparison. As the bead ratio increases, the geometry of the beaded-panel configuration approaches a configuration that resembles the blade-stiffened panel, yet is more structurally efficient. Since the stiffeners are formed from thin sheets, the material is more efficiently used to support the loads by placing it away from the reference surface in an effective manner. The cross-sectional geometries of the beaded hat-stiffened panel are shown in Fig. 15. Again, the bead-stiffened panel geometry resembles the geometry of the optimum blade-stiffened panel. Design trends similar to the ones for the bead-stiffened panels loaded in axial compression only are observed for bead-stiffened panels with combined axial compression and shear loads. Each configuration resembles the design of the optimum blade-stiffened panel geometry for the given load combination.

The results of the study suggest that when a corrugated-type panel is formed into a bead-stiffened panel, it can perform similarly to (if not better than) a blade-stiffened panel, with potential reductions in the manufacturing and fabrication costs of the panel. Further analytical study and experimental evaluation are necessary, however, to fully assure the applicability and cost-effectiveness of this type of configuration.

*Blade-Stiffener Spacing*

To understand better the effects of large stiffener spacing on the design, optimum stiffener spacing trends are considered first. The trends of the optimum stiffener spacing of blade-stiffened panels under combined axial compression and shear are shown in Fig. 16. The optimum blade spacing for light axial compression loads is large compared to the panel width of 80 in. For $N_x/L = 1.0$ psi, e.g., the optimum spacing is about 12.5 in. As the ratio of the shear load to axial compression load is increased for a constant axial compression load, the stiffener spacing is reduced slightly to account for the additional load. For example, for a ratio of $N_{xy}/N_x = 1.0$, with $N_x/L$ near 1.0 psi, the stiffener spacing is reduced to 8.5 in. As the axial compression loads increase to a moderate value (near 100 psi), the stiffener spacing decreases and reaches its minimum value of 3 in. (2 in. for $N_{xy}/N_x = 1.0$). For axial compression load values greater than $N_x/L = 200$ psi, the minimum-gauge constraint becomes inactive and both the stiffener spacing and stiffener size increase steadily with the axial load, reaching a stiffener spacing of about 5 in. for $N_x/L = 1000$ psi. The change in the optimum blade-stiffener spacing due to additional shear loading is relatively small for $N_x/L = 1000$ psi. In general, the optimum blade-stiffener spacing is a strong function of load level. If the minimum-gauge constraint is active, the blade stiffeners remain small and closely spaced. Once the minimum-gauge constraint becomes inactive, near $N_x/L = 200$ psi, larger stiffeners are needed to carry the load, and they are spaced farther apart.

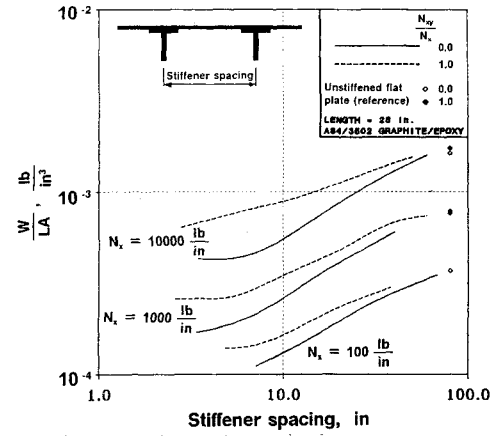


**Fig. 17 Effect of stiffener spacing on blade-stiffened panel weight with axial compression ($N_x$) and shear ($N_{xy}$) loads.**

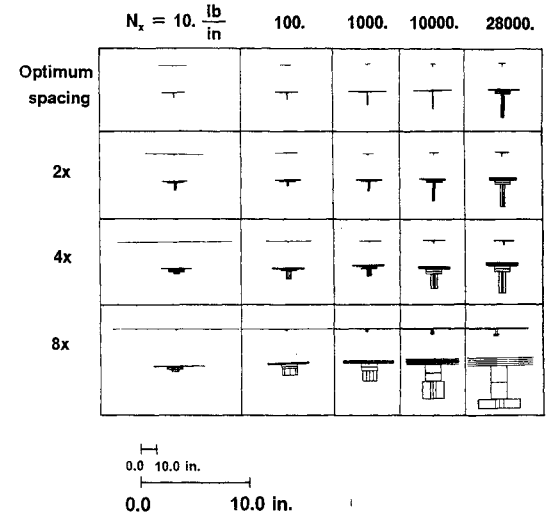


**Fig. 18 Effect of nonoptimum stiffener spacing on compression-loaded blade-stiffened panel.**

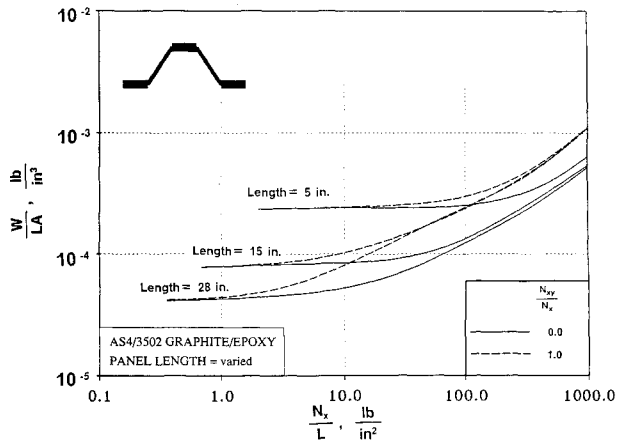


**Fig. 19 Effect of panel length on structural efficiency of the tailored corrugated panel.**

The distance between the stiffeners is increased in multiples of the optimum stiffener spacing until the spacing between two adjacent blade stiffeners approaches the panel width of 80 in. Results for load cases with axial compression ($N_x = 100$, 1000, and 10,000 psi) and shear ($N_{xy}/N_x = 0.0$ and 1.0) are shown in Fig. 17. Large changes in the stiffener spacing cause a significant increase in the structural weight that approaches the weight of an unstiffened flat plate indicated by symbols in Fig. 17 for stiffener spacing approaching the panel width. The corresponding blade-stiffener geometries change significantly for the nonoptimum spacing and are shown in Fig. 18 for various load levels. The stiffener appears to approach a Tee-stiffener configuration for spacings on the order of eight times the optimum spacing. Since the initial PASCO model is intended to be used for blade-stiffened panels (the flange width of the blade stiffener is constrained to be 1.5 in. wide, and the laminate in the blade itself is oriented perpendicular to the skin), the use of the same model for Tee-stiffened panels may be inappropriate. The high load level and large stiffener spacing, which cause this drastic configuration change, suggest that a stiffener configuration other than the blade may be more suited for these extreme cases with these unrealistic constraints.

### Length Effects

The effect of panel length on weight is shown in Fig. 19 for the tailored corrugated panel. Panel lengths of 5, 15, and 28 in. are considered. For load levels below $N_x/L = 100$ psi, the structural efficiency of the panels appears to degrade as the length is shortened. However, the minimum-gauge ply thickness constraint is active in this load range for all three lengths considered, and the panels are made up of essentially the same thickness laminates, based on the number of plies needed to define the laminate in the model. The same holds true for the hat-stiffened panel. For the lightly loaded panels, this observation leads to the conclusion that the weight per unit area of the panel is the same, regardless of the length. Since the weight index is defined in this study as the weight per unit area over the length, a $1/L$ factor causes the discrepancy between different length panels. As $N_x/L$ increases above 100 psi, the weight index of the panels with different lengths approaches a common value. As discussed earlier, the material-failure criterion is active for highly loaded panels.

### Layup Changes

The PASCO models used in the present design study are based on many practical considerations such as using a continuous laminate with $\pm 45$-, 0-, and 90-deg plies for the corrugation, or using a continuous $\pm 45$-deg laminate with 0-deg plies added to the caps of the corrugation for the tailored corrugated and the hat-stiffened panels. To assess the effect of variations in the panel laminates on structural efficiency and cross-sectional geometry, a study was conducted in which 0-deg plies were added to the tailored corrugated panel web laminate, and the results of this study are presented in the following section.

*Corrugated Webs with 0-Deg Plies*

Tailored corrugated and hat-stiffened panels are redesigned for various loads after including an independent 0-deg ply variable without a minimum-gauge limit in the web laminate. The effect of the added 0-deg plies on the panel geometry becomes somewhat significant for axial compression load levels above 200 psi, where the minimum-gauge constraint in the overall design is no longer active. There are slight changes in the cross-sectional geometry of these designs which do not affect the weight of either the tailored corrugated panel or the hat-stiffened panel. PASCO determines the load distribution in the cross section by assuming a constant strain throughout the panel width; therefore, the addition of 0-deg plies to the web significantly increases the local load carried by the web due to the increased stiffness of the web. Much of that load, however, is carried by the 0-deg plies, and the thickness requirement of the $\pm 45$-deg plies in the web laminate is reduced relative to the thickness of $\pm 45$-deg plies in the laminate without the 0-deg plies. Since the $\pm 45$-deg plies are continuous throughout the panel (although they are mostly required in the web laminate), a reduction in the $\pm 45$-deg ply thicknesses required in the web causes a significant reduction in weight, which offsets the weight increase due to the added 0-deg plies.

*Discrete Ply Thicknesses*

An important practical consideration for composite panel designs is the availability of material in discrete ply thicknesses. PASCO sizes the individual ply thicknesses by allowing them to change continuously and to assume any value within the specified bounds. Since a laminated composite panel can only be fabricated from plies with discrete thicknesses, typically 0.005 in. thick, the effect of rounding the optimum ply thickness design variables up to the nearest discrete ply thickness on structural efficiency and geometry was studied, and the results of the study are presented in this section. The panel configurations with optimized thickness design variables were redesigned after fixing the ply thicknesses to the next highest discrete value available to obtain the optimum geometry for the new discrete ply thickness design. Only small changes in the panel geometry were observed for all of the configurations studied, and there were only negligible weight increases.

## Concluding Remarks

The results of a structural-efficiency study on several graphite-epoxy rib concepts for a typical transport wing are presented. The effects of varying loading intensities on structural weight and rib geometric parameters are compared for corrugated panels, hat- and blade-stiffened panels, and unstiffened flat panels. The panels are subjected to various combinations of axial compression, in-plane shear, and out-of-plane normal pressure loadings typical of rib structures. Minimum-weight designs that satisfy buckling, strength, and minimum-gauge design constraints have been obtained using the PASCO panel analysis and sizing computer code. Unconservative PASCO shear buckling calculations have been improved with the more accurate shear buckling analysis capability in the VICON computer code.

Results for panels loaded in axial compression alone indicate that a tailored corrugated panel concept with different laminates in the corrugation crowns and webs is the most structurally efficient configuration for lightly loaded ribs. A corrugated panel concept with a continuous or uniform lami-

nate in the corrugation crowns and webs is the next most structurally efficient concept, followed by the blade-stiffened panel concept, the hat-stiffened panel concept, and the unstiffened flat panels. As the axial compression load intensity increases, the weight of the blade-stiffened panel concept increases more rapidly than the other concepts, and it becomes the heaviest configuration.

Adding an out-of-plane pressure load to panels that are also loaded in axial compression has the most pronounced effect on the structural efficiency and cross-sectional geometry of panels loaded in the low axial compression load range. For all of the configurations studied with low values of axial compression loads, a pressure load causes significant weight increases that are associated with increased stiffener height and more closely spaced stiffeners. The weight increases more slowly, however, as the intensity of the pressure load increases. The weight increase due to pressure load for the hat-stiffened panels is small compared to that of the corrugated panels. For panels loaded by high values of axial compression loads, a pressure load only has a minor effect on structural weight, although some changes in the cross-sectional geometries occur.

For all configurations studied, combinations of in-plane shearing loads with axial compression loads result in little change in structural efficiency at the lower axial compression load levels where minimum-gauge constraints are dominant. As the compression load intensity increases, buckling constraints dominate the design and cause significant weight increases compared to panels loaded by axial compression alone. In general, combined compression and shear loads affect the geometric parameters of minimum-weight designs differently than panels designed for compression or shear loads alone.

It was found that imposing changes in optimum stiffener spacing or other optimum geometric parameters influences both structural efficiency and cross-sectional geometric details of the configurations studied. Forcing a large spacing between the corrugations of a corrugated panel creates a new configuration that is similar to a bead-stiffened panel concept. The structural performance of bead-stiffened panels is shown to be similar to that of a blade-stiffened panel. In addition, the bead-stiffened panel concept may be suitable for cost-effective manufacturing procedures, such as thermoforming of thermoplastics. Forcing an increased spacing between the stiffeners of a blade-stiffened panel causes a large increase in weight and changes the cross-sectional geometry significantly. The resulting configuration is similar to that of a Tee-stiffened panel, suggesting the possibility of a more suitable configuration for these extreme cases. The results of this preliminary study also indicate that changes in optimum laminates have a small effect on structural efficiency if other design variables are free to change. In addition, it was found that panel length influences the structural efficiency of lightly loaded panels dominated by minimum-gauge constraints.

## References

[1]Swanson, G. D., "Structural Efficiency of Composite Wing Rib Structures," M.S. Thesis, Virginia Polytechnic Inst. and State Univ., Blacksburg, VA, Feb. 1988.

[2]Anderson, M. S., Stroud, W. J., Durling, B. J., and Hennessy, K. W., "PASCO: Structural Panel Analysis and Sizing Code, User's Manual," NASA TM-80182, Nov. 1981.

[3]Stroud, W. J., and Anderson, M. S., "PASCO: Structural Panel Analysis and Sizing Code, Capability and Analytical Foundations," NASA TM-80801, Nov. 1981.

[4]Wittrick, W. H., and Williams, F. W., "Buckling and Vibration of Anisotropic or Isotropic Plate Assemblies under Combined Loadings," *International Journal of Mechanical Sciences*, Vol. 16, April 1974, pp. 209–239.

[5]Vanderplaats, G. N., "CONMIN—A Fortran Program for Constrained Function Minimization, User's Manual," NASA TM X-62, 282, 1973.

[6]Stroud, W. J., Greene, W. H., and Anderson, M. S., "Buckling Loads of Stiffened Panels Subjected to Combined Longitudinal Compression and Shear: Results Obtained with PASCO, EAL, and STAGS Computer Programs, " NASA TP-2215, Jan. 1984.

[7]Williams, F.W., and Kennedy, D., "User's Guide to VICON, VIPASA with Constraints," Dept. of Civil Engineering and Building Technology, Univ. of Wales Inst. of Science and Technology, Aug. 1984.

[8]Williams, F. W., and Anderson, M. S., "Incorporation of Lagrangian Multipliers into an Algorithm for Finding Exact Natural Frequencies or Critical Buckling Loads," *International Journal of Mechanical Sciences*, Vol. 25, No. 8, 1983, pp. 579–584.

[9]Stroud, W. J., and Agranoff, N., "Minimum-Mass Design of Filamentary Composite Panels under Combined Loads: Design Procedure Based on Simplified Buckling Equations," NASA TN D-8257, 1976.

[10]Stroud, W. J., Agranoff, N., and Anderson, M. S., "Minimum-Mass Design of Filamentary Composite Panels under Combined Loads: Design Procedure Based on a Rigorous Buckling Analysis," NASA TN D-8417, July 1977.